Electronic Supplementary Material (ESI) for Lab on a Chip.

Supporting Information

Simultaneous Electrical Recording of Cardiac Electrophysiology and Contraction on Chip

Fang Qian,[a‡] Chao Huang,[b‡] Yi-Dong Lin,[c‡] Anna N. Ivanovskaya,[b] Thomas J. O'Hara,[a] Ross H. Booth,[b] Cameron J. Creek,[b] Heather A. Enright,[a] David A. Soscia,[b] Anna M. Belle,[b] Ronglih Liao,[c] Felice C. Lightstone,[a] Kristen S. Kulp[a,*] and Elizabeth K. Wheeler[b,*]

[a] Physical and Life Science Directorate, Lawrence Livermore National Laboratory, Livermore, California 94550, U.S.A.

[b] Engineering Directorate, Lawrence Livermore National Laboratory, Livermore, California 94550, U.S.A.

[c] Department of Medicine, Harvard Medical School/Brigham Women's Hospital, Boston, Massachusetts 02115, U.S.A.

Corresponding authors: wheeler16@llnl.gov (Tel: +1-925-423-9722); kulp2@llnl.gov (Tel: +1-925-422-6351)

Electrochemical characterization and modelling of different IDE geometries

Four different IDE geometries were designed with systematically increased sizes (Fig. S1). Details on geometry factors of fabricated IDE structures A-D are summarized in Table S1. Characterization of fabricated IDE assemblies was performed by electrochemical impedance spectroscopy (EIS) inside 100 μS/cm conductivity standard solution (0.00068 M KCl, Alfa Aesar). Two-electrode cell arrangement was used for the impedance measurement. Leads of potentiostat equipped with EIS (SP-300 with low-current channel option, Bio-Logic Inc.) were connected between two electrodes of IDE assembly. Measurement was performed for a frequency range 100 Hz to 3 MHz with 10mV oscillation amplitude under open circuit conditions.

Impedance spectra measured in 100 μS/cm conductivity standard (CS) solutions on fabricated IDE are shown in Fig.S2. Measured curves were fitted with equivalent circuit model composed of four elements: $R_\Omega + R_s/C_p + Q$, where R_Ω is trace resistance, R_s is solution resistance, C_p is capacitance of traces and IDE and Q is constant phase element representing double layer capacitance at the electrode-solution interface [1]. Quality of fit was found to be good over the entire range of frequencies used for the tests. Summary of parameters extracted from data fits are shown in Table S2. For A and B structures averaged values and standard deviations were extracted form testing of several identical assemblies. CPE parameter Q was found to scale linearly with geometric area of the electrodes as it is expected for capacitance of double layer formed at electrode-solution interface. Alpha parameter is close to experimentally observed values for platinum electrodes in chloride containing solutions [2]. Solution resistance R_s and capacitance C_p values were compared to theoretical values derived from cell constants calculated for each structure. Capacitance and solution resistance where calculated from cell constants of IDE assemblies using the following relations: $K = R_s \sigma = \frac{\varepsilon_0 \, \varepsilon_r}{C_p}$ (where σ conductivity of KCl solution 100 μS/cm, ε_0 is vacuum permittivity and ε_r is relative permittivity of KCl solution taken as 78.3 from literature [3]. For basic IDE geometries, cell constant can be calculated from geometry according to the following equation (where S is inter-trace distance, W and L are finger width and length and N is number of fingers in IDE):

$$K = 2\frac{\sqrt[3]{S/W}}{L(N-1)} \qquad [4,5]$$

For IDE structures composed of several IDE cells (n) connected in parallel cell constant diminishes n times compared to that of the unit cell (K/n).

Capacitance C_p for geometry A was found to be dominated by capacitance of leads (in order of 8 pF) that is in parallel to the capacitance of IDE. Capacitances of IDE assemblies (after correction by subtracting capacitance of leads) deviate from theoretical calculations by not more than 30% (Fig. S3a). Cell constants extracted from measurement and from calculations are shown on Figure S3b. For the most of the cells, cell constants from measurements are lower that from calculation. This type of mismatch was previously reported for variety of IDE geometries and attributed to fringing effects at dielectric-solution interface in the vicinity of electrodes. Among all tested structures measured cell constant for geometry A deviates from theoretical the most (by 40%). It is expected that the formula for cell constant is more accurate in case of longer IDE fingers as compare to the shorter ones [4].

Extraction of tissue layer resistance and capacitance from Nyquist plots

Properties of tissue layer were extracted from EIS spectra using the following methods. Since tissue impedance can be considered connected in series with that of the device coated with protein, to obtain tissue impedance, measured spectra for device coated with protein layer (Z_0) was subtracted from that of the device with protein and cells (Z_1) as following: Re Z = Re Z_1 – Re Z_0; Im Z = Im Z_1 – Im Z_0. Nyquist plots at high frequencies (26 kHz – 3 MHz) after subtraction resemble semicircles (typical Nyquist plot for DIV-4 is shown on Fig. S4) confirming that equivalent circuit model for the tissue layer can be considered simply as a resistance in parallel with a capacitance. The resistance of the tissue was extracted from Nyquist plots from intersect of the semicircle with X-axis (85 Ω for DIV-4) and tissue capacitance (6.7 nF for DIV-4) was calculated from frequency f^* at maximum Y value (278 kHz) from equation $2\pi f^* RC = 1$. Comparison of optimal frequency for cardiac activity (30 kHz) with frequency range of EIS spectra (Fig. S4), suggests that since 30 kHz is within the range of frequency where impedance of the tissue rather that double layer capacitance governs the response, changes in tissue layer properties (increase in resistance or decrease in capacitance) were mainly responsible for observed increase in impedance during beating.

References

[1] “Impedance Spectroscopy: Applications to Electrochemical and Dielectric Phenomena”, by Vadim F. Lvovich, ISBN: 978-0-470-62778-5.

[2] “Impedance Characterization and Modeling of Electrodes for Biomedical Applications”, Wendy Franks, Iwan Schenker, Patrik Schmutz and Andreas Hierlemann*, IEEE TRANSACTIONS ON BIOMEDICAL ENGINEERING,* 52, pp.1295 (2005)

[3] “Absorption and Drug Development: Solubility, Permeability, and Charge State”, by Alex Avdeef, ISBN: 978-1-118-05745-2.

[4] “Theoretical and experimental determination of cell constants of planar-interdigitated electrolyte conductivity sensors” W. Olthuis, W. Streekstra, P. Bergveld, *Sensors and Actuators B: Chemical*, 24, pp.252 (1995)

[5] Mosaic Industries website at http://www.mosaic-industries.com/embedded-systems/instrumentation/conductivity-meter/microfabricated-planar-interdigitated-electrodes-cell-constant

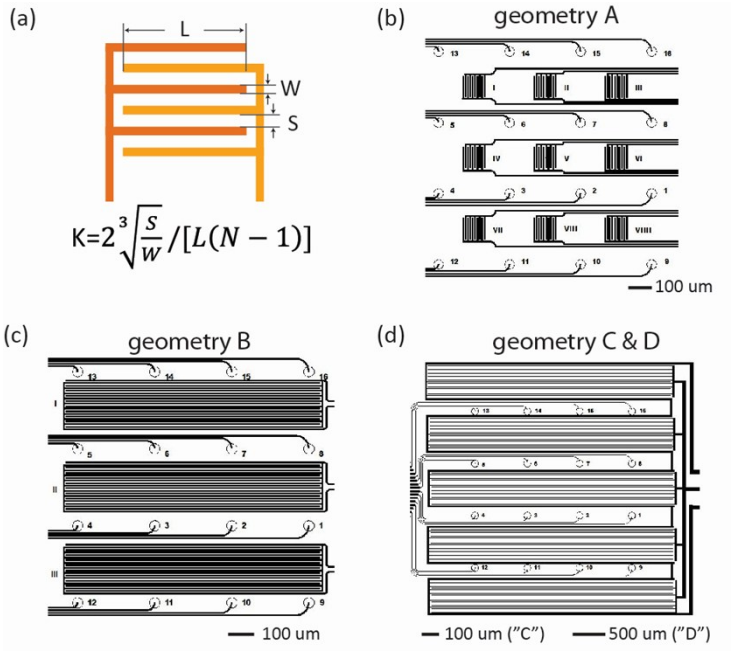

Figure S1. (a) A schematic showing a basic IDE structure used as a unit cell for IDE structure design. (b-d) Schematics of the electrode design in the four geometries. Geometry A is a nine-IDE array, B is a three-IDE array, C and D are serially-connected IDE assembly of different dimensions.

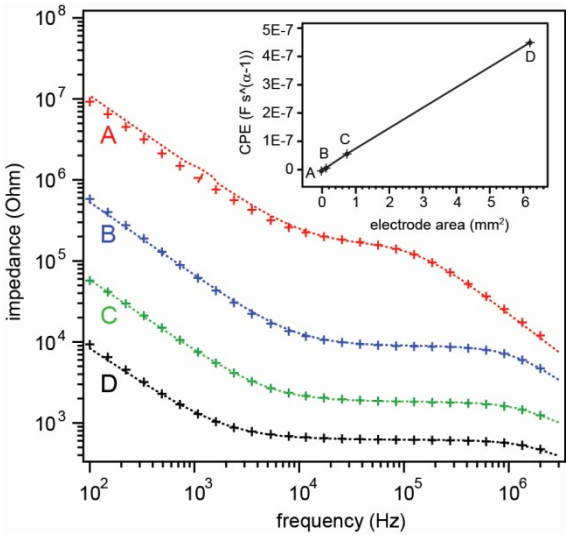

Figure S2. EIS measured with A (red), B (blue), C (green) and D (black) structures in 100 μS/cm conductivity standard. Experimental data (crosses) is shown together with data fit with $R_{trace} + R_s/C_p + Q$ equivalent circuit model (dotted lines). Inset: CPE extracted from EIS data in 100 μS/cm CS as a function of electrode area. Inset: Plot confirms expected linear dependence.

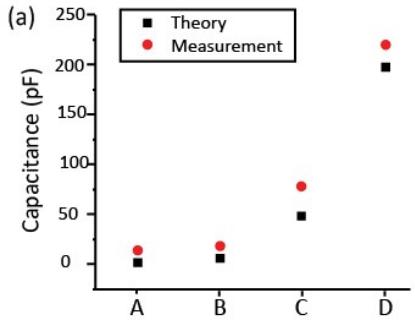

(b)

IDE structure	Calculated K (1/cm)	Measured K (1/cm)	Deviation from theory (%)
A	25.25	15.40	39
B	1.06	0.86	19
C	0.144	0.124	14
D	0.036	0.038	11

Figure S3. (a) Capacitance of devices derived from theory and C_p obtained from EIS data fit. (b) Comparison of electrochemical cell constants (K) derived from experimental results (R_s) with theoretical calculations.

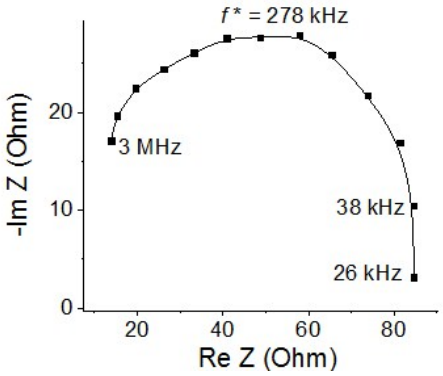

Figure S4. A representative Nyquist plot collected from DIV-4 cardiac tissue.

Table S1. The parameters of the four IDE geometries

IDE structure	# of fingers	Finger length, μm	Overlay length, μm	Finger width, μm	Interspace, μm	# of IDE cells	Electrode area, cm^2
A	10	100	88	5	5	1	5.00E-05
B	20	1000	990	5	5	1	1.00E-03
C	21	1400	1390	5	5	5	7.35E-03
D	31	4000	3806	10	10	5	6.20E-02

Table S2. Parameters extracted from fitting EIS data with equivalent circuit model

IDE structure	Rs, Ohm	Cp, pF	Q, $F\ s^{\alpha-1}$	α	R trace, Ohm
A	144 100 ± 5 720	8.2 ± 0.5	$(2.76 \pm 0.5) \times 10^{-10}$	0.9 ± 0.01	598 ± 141
B	8 582 ± 18	15 ± 0.3	$(5.35 \pm 1.8) \times 10^{-9}$	0.91 ± 0.03	226 ± 97
C	1 238	78.09	55.5×10^{-9}	0.89	576
D	373.3	220.7	4.49×10^{-7}	0.87	244

Cardiac Simulation Methods

The Paci cell model [1] was implemented in Matlab (The MathWorks, Inc., Natick, MA, USA) using the "ode15s" coupled differential equation solver. No stimulus current was delivered, allowing spontaneous firing only, during a window of 10 sec. The effect of norepinephrine (NE) application was simulated using the same changes to target proteins used previously in human adult ventricular cell simulations based on the Heijman model of β-adrenergic signaling [2,3]. The Paci iPS model includes the "funny" current (encoded by HCN4), which is not found in ventricle, and so the β1 response required a novel definition: 2-fold increase in conductance, in accord with experiments [4].

We simulated 16 individual cells to represent measurements from the 16 MEA electrodes on the chip device. Cell-to-cell variability was established by altering the maximum conductance of the 14 ion channel currents/fluxes from the original Paci values (pseudo-random multiplicative factors were drawn from a normal distribution using the "randn" function in Matlab). Ten simulated chip trials were performed for each of seven different specifications of variability (standard deviation about the mean = 0.01, 0.05, 0.1, 0.25, 0.333, and 0.5 corresponding to 1, 5, 10, 25, 33.3, and 50% cell-to-cell variability, respectively). Trials were repeated six times to ensure repeatability of findings.

Initial Paci model state (resting values, used in all simulations):
v = -0.0743340057623841
m = 0.102953468725004
h = 0.786926637881461
j = 0.253943221774722
d = 8.96088425225182e-5
f1 = 0.970411811263976
f2 = 0.999965815466749
fCa = 0.998925296531804
Xr1 = 0.00778547011240132
Xr2 = 0.432162576531617
Xs = 0.0322944866983666
Xf = 0.100615100568753
q = 0.839295925773219
r = 0.00573289893326379
Nai = 10.9248496211574
Cai = 1.80773974140477e-5
Ca_SR = -0.2734234751931
g = 0.999999981028517

References

[1] Paci M, Sartiani L, Del Lungo M, Jaconi M, Mugelli A, Cerbai E, et al. *Biomed Eng Online*, 2012, **11**: 61.
[2] O'Hara TJ, Rudy Y. *Hear Rhythm*, 2012, **9,** 275.
[3] Heijman J, Volders PGA, Westra RL, Rudy Y. *J Mol Cell Cardiol.* 2011, **50**, 863.
[4] Greene D, Kang S, Kosenko A, Hoshi N. *J. Biolog. Chem.* 2012, **287**, 23690.

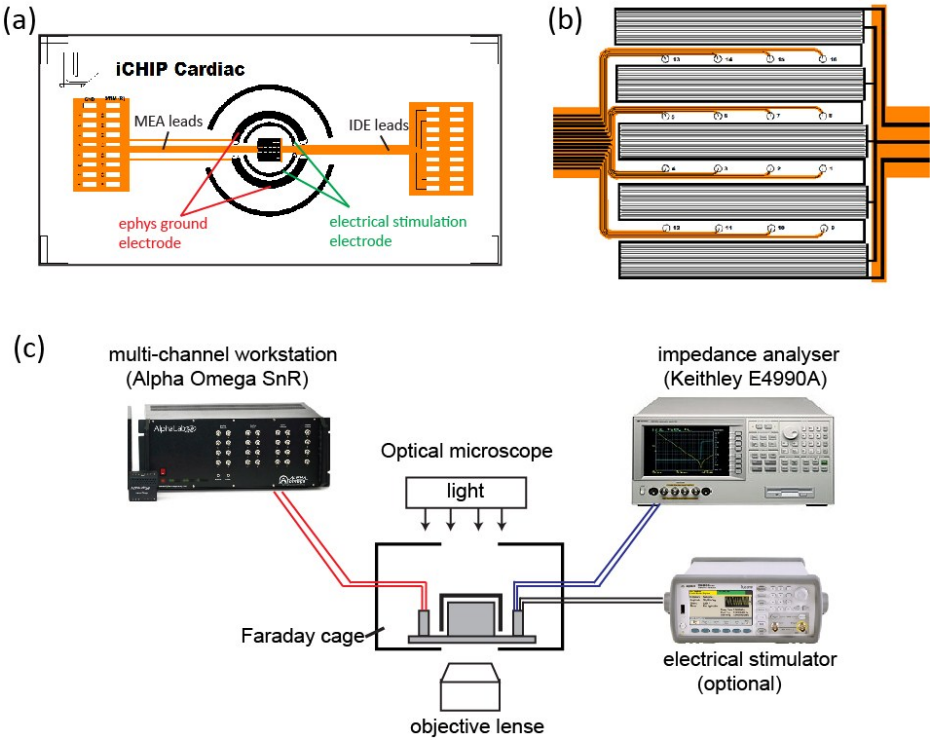

Figure S5. Chip design and experimental setup. (a,b) The overall 30 mm x 15 mm chip design includes the MEA array, the IDE array, ground electrodes, electrical stimulation electrodes, leads to the external Omnetic connectors. Electrodes are Ti/Au thin films (black color) and passivation layer is polyimide (orange). (c) Measurement setup and instruments.

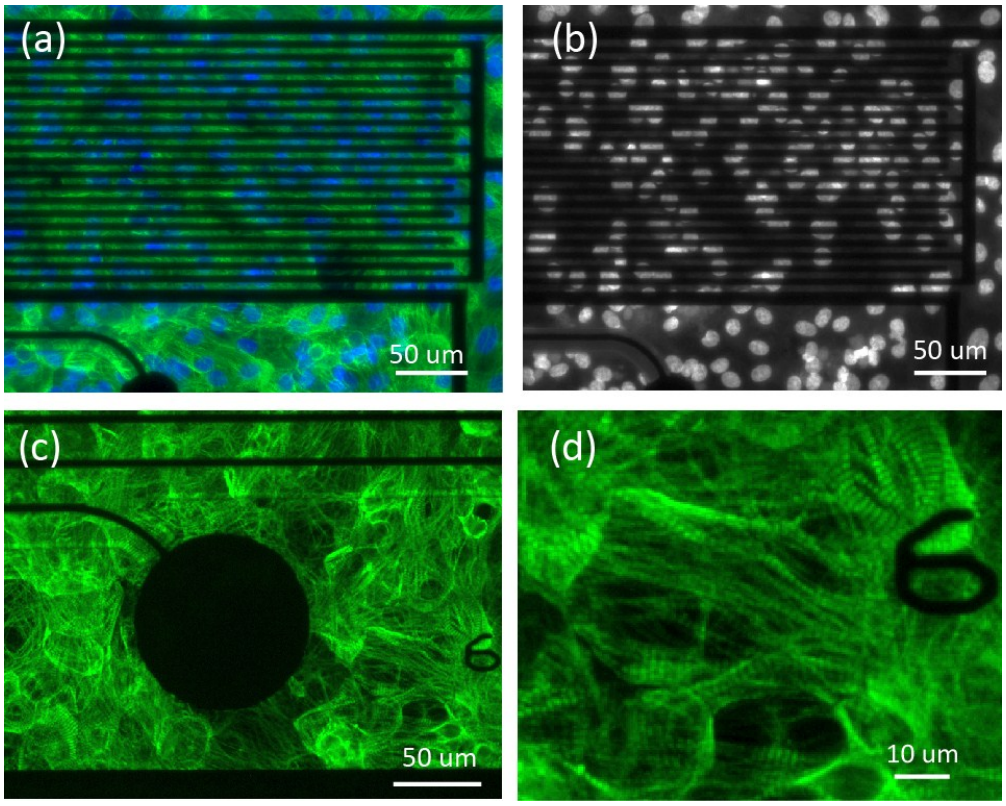

Figure S6. Immunofluorescence images taken from cardiac tissues grown on geometry D. (a) A fluorescence images of hiPS CM tissues cultured on the device, stained by Hoechst (blue) and cTnT (green). (b) The fluorescence image of hiPS CMs stained by Hoechst. The image was taken from the same region of (a). Note nuclei can be clearly seen through the IDE so that cell numbers can be quantified if needed. (c, d) High-resolution fluorescence images of cells stained by cTnT (green). Well-defined sarcomere segments were clearly resolved.

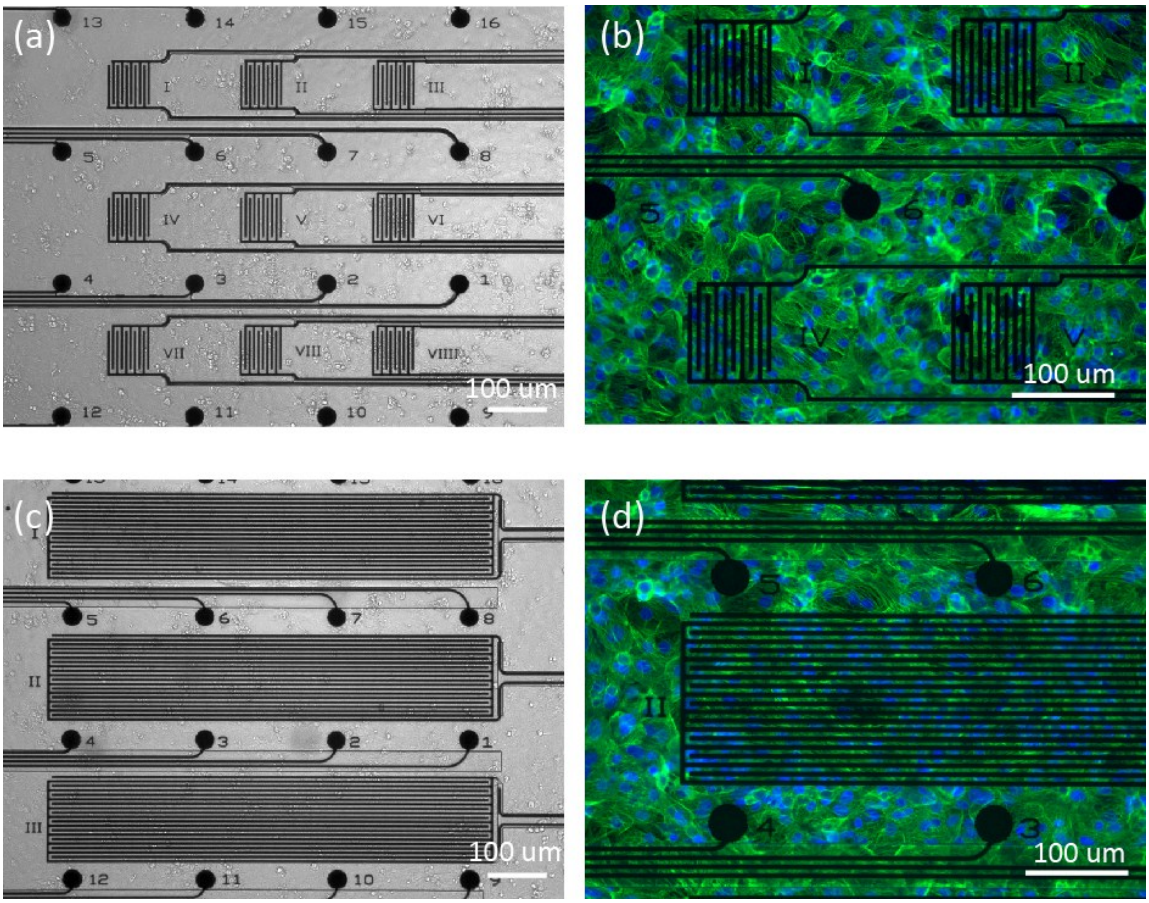

Figure S7. Cardiac tissues cultured on geometry A (a,b) and geometry B (c, d) showed similar platform biocompatibility. Blue color shows nuclei stained by Hoechst and green color shows troponin stained by cTnT.

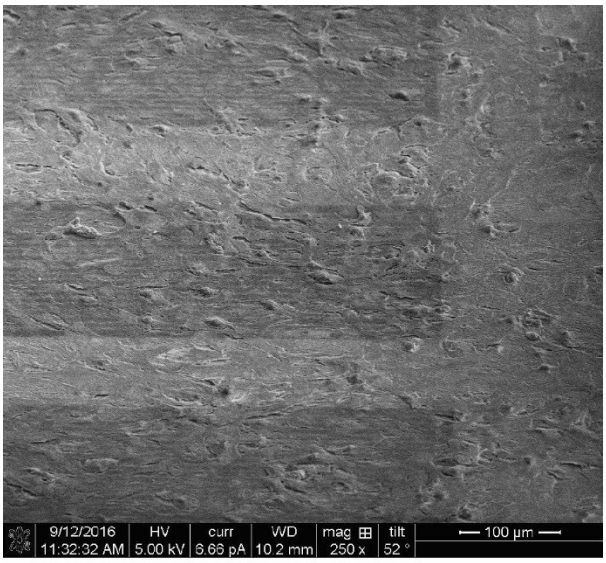

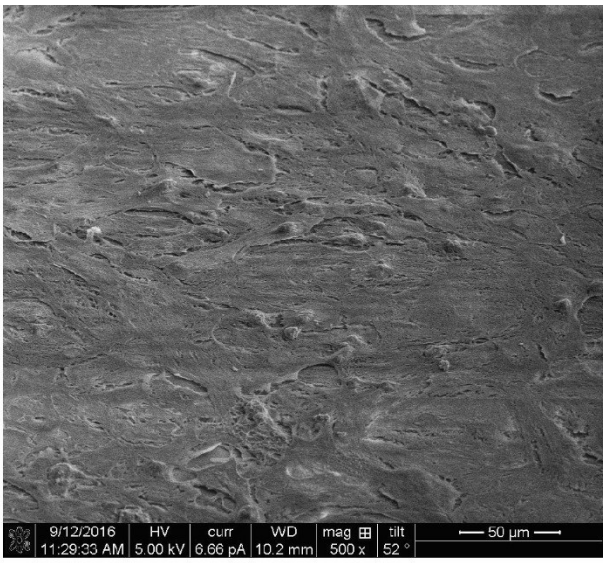

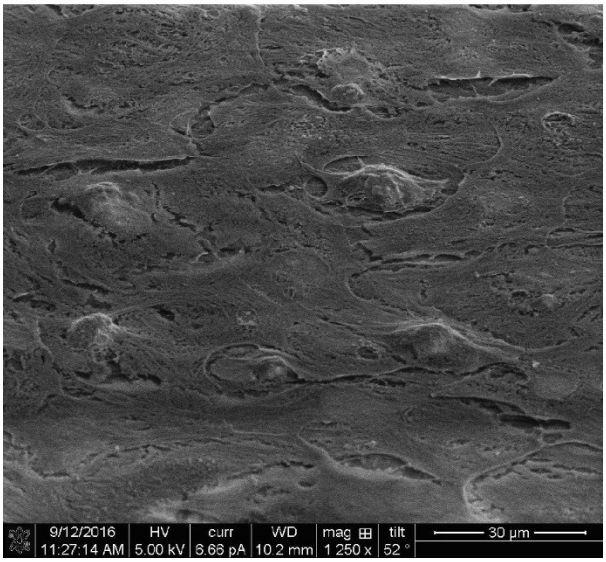

Figure S8. More SEM images showing full coverage of hiPS-CMs uniform monolayer over the entire device surface.

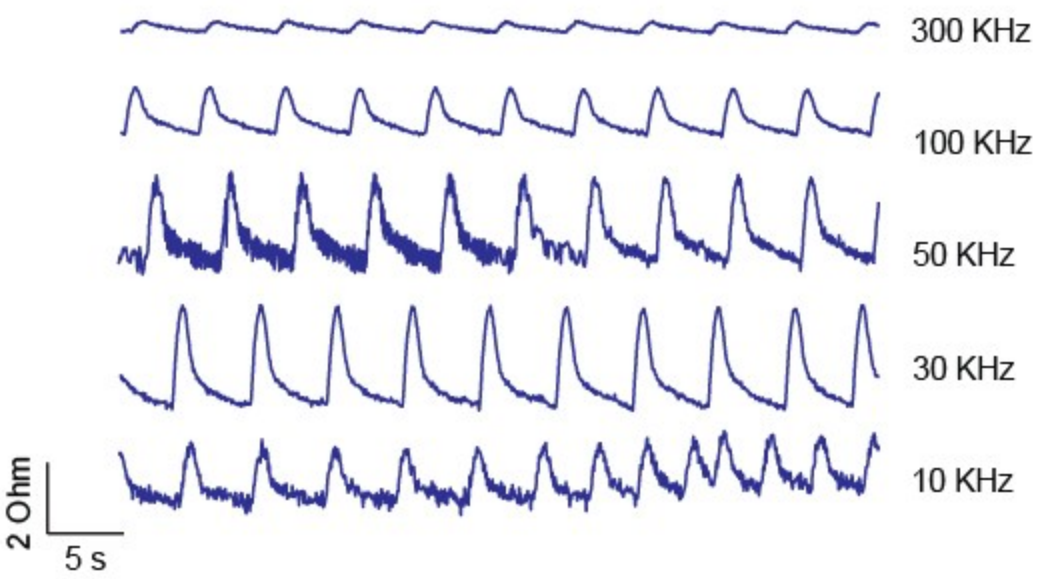

Figure S9. Impedance vs time plot of cardiac contraction as a function of frequency. Signal-to-noise ratio increased with frequency and reached maximum at f=30 kHz, then decrease at higher frequencies. Some curves exhibited ascending baseline drift because temperature hasn't been stabilized to room temperature.

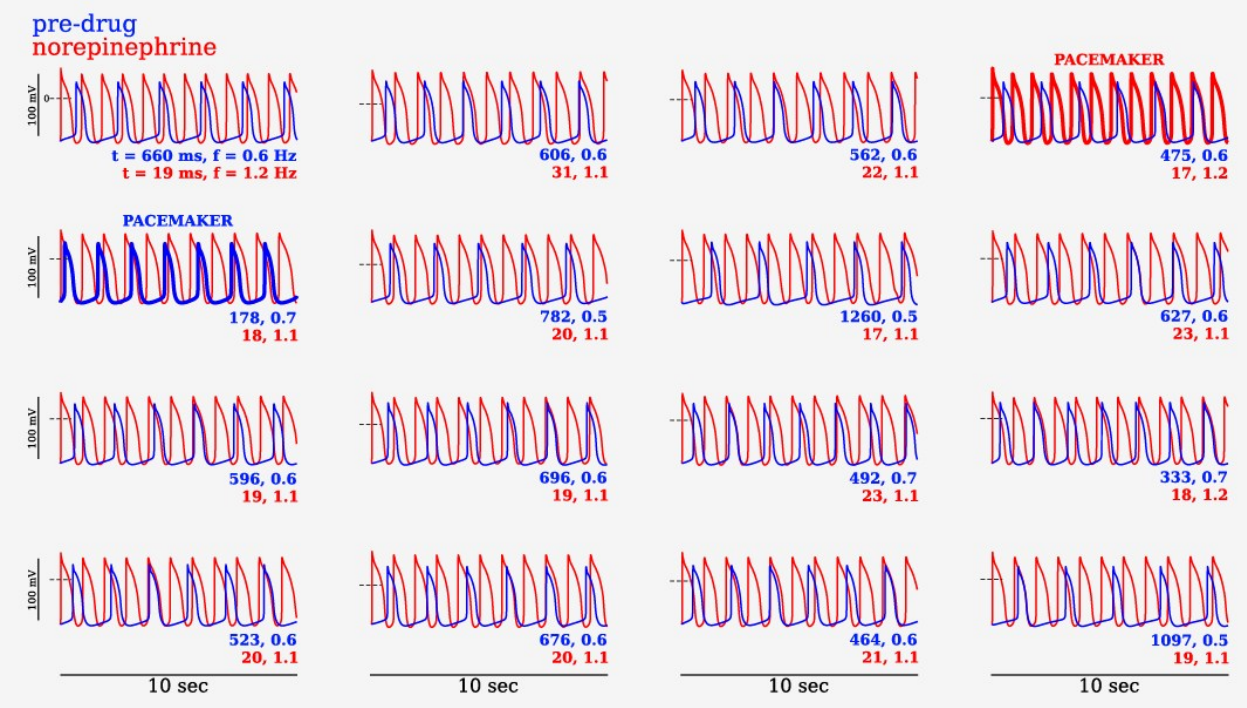

Figure S10. Inherent cell-to-cell variability can account for a change in pacemaker following norepinephrine (NE) application. Shown are example simulated Paci *et al.* action potentials (membrane voltage versus time) under control conditions (blue, pre-drug) and with NE (red). Cell-to-cell variability was 10% in this example. Time to first AP (t) and pacing rate (f) are displayed below traces. The pacemaker was defined as the cell with both the fastest automatic pacing rate that also was first to excite. The cell with these properties, the pacemaker, changed following simulated NE application (bolded traces and "PACEMAKER" label).

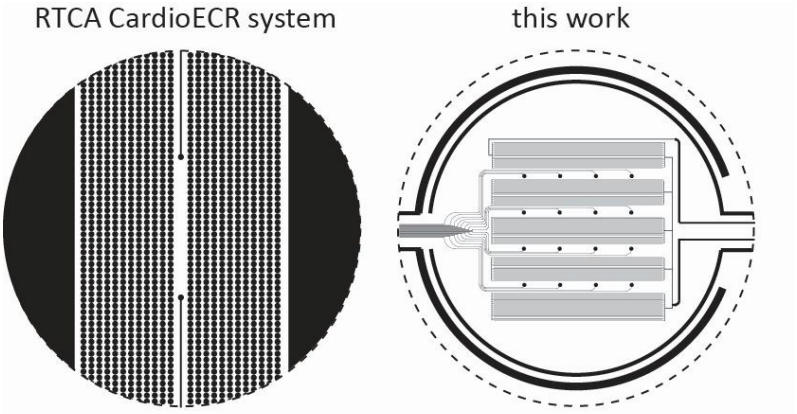

	RTCA CardioECR system	this work
device size	~6.35 mm (compatible with 96-well plates)	~6.35 mm (compatible with 96-well plates)
# of MEA	2	16
diameter of MEA electrode	ca. 150 um	40 um
line-width of IDE electrode	ca. 150 um	5 um
transpareny	~ 35%	~ 85%
stim electrode	N/A	Yes

Figure S11. Comparison of this work with RTCA CardioECR® systems. The schematics are drawn to scale. The geometry parameters of RTCA CardioECR system® were extracted from reference #12 and #13. The transparency of the device was estimated by measuring the black-to-white ratio of the design schematics using ImageJ software.

Supplementary movies #1, #2. hiPSC CMs formed a uniform monolayer on device, beating spontaneously and in synchronization.

Supplementary movie #3. Electrical pacing of primary rat cardiomyocytes (Clonetics™ Rat Cardiac Myocytes, Lonza Walkersville Inc., Walkersville, MD), which did not exhibit spontaneous beating. Duration from 0 to 20 sec: no stimulation; from 20 to 50 sec: electrical pacing at 4V (peak to peak amplitude) with a frequency of 0.2 Hz; from 50 to 72 sec: no stimulation.